Tumorigenesis and Neoplastic Progression

Re: AJP10-0745 Version 2

RANKL expression specifically observed *in vivo* promotes epithelial mesenchymal transition and tumor progression

Tamaki Yamada,[*†‡], Masumi Tsuda,[*] Tomomi Takahashi,[†] Yasunori Totsuka,[‡] Masanobu Shindoh,[†] and Yusuke Ohba[*]

From the Laboratory of Pathophysiology and Signal Transduction, Hokkaido University Graduate School of Medicine,[*] Sapporo; Division of Oral Pathobiological Science[†] and Laboratory of Oral and Maxillofacial Surgery,[‡] Hokkaido University Graduate School of Dental Medicine, Sapporo, Japan.

This manuscript consists of 31 pages, 1 table, and 7 figures.

Running Title: RANKL promotes EMT and tumor progression *in vivo*

Supported in part by grants-in-aid from the Ministry of Education, Culture, Sports, Science and Technology, Japan and the Japan Society for Promotion of Science, and grants from the Japan Science and Technology Agency, Akiyama Foundation, and the Mochida Memorial Foundation for Medical and Pharmaceutical Research.

None of the authors disclosed any relevant financial relationships.

Address reprint requests to Yusuke Ohba, M.D., Ph.D., Laboratory of Pathophysiology and Signal Transduction, Hokkaido University Graduate School of Medicine, N15W7, Kita-ku, Sapporo 060-8638, Japan. Tel.: +81-11-706-5158; fax: +81-11-706-7877; E-mail: yohba@med.hokudai.ac.jp

Abstract

Recent findings focus much attention on the molecular consequence of the microenvironment in tumor progression; nonetheless, events occurring in cancer cells themselves in response to their ambient conditions remain obscure. Here, we identify receptor activator of nuclear factor κB ligand (RANKL) as a microenvironment-specific factor essential for tumorigenesis *in vivo*, utilizing head and neck squamous cell carcinoma (HNSCC) as a model. In human HNSCC tissues, RANKL is abundantly expressed, and its expression level correlates with the histological grade of differentiation. In fact, RANKL levels are significantly higher in poorly differentiated SCCs than those in well- or moderately differentiated SCCs. In contrast, all HNSCC cell lines tested display extremely low RANKL expression, which is, however, efficiently upregulated when these cell lines are inoculated in the head and neck region of mice. This restored RANKL expression is in a microenvironment-specific manner, and cannot be observed when the cells are inoculated in the hindlimbs. Interestingly, forced expression of RANKL compensates for tumor growth in the hindlimb milieu, promotes epithelial mesenchymal transition (EMT), and induces tumor angiogenesis, in a manner independent of VEGF. These results implicate RANKL expression causatively in tumor growth and progression in HNSCC *in vivo*, and may therefore provide a novel functional marker for biological malignancy and a therapeutic target based on the specific nature of the microenvironment.

Introduction

The microenvironment — the sanctuary in which a tumor originates — plays a critical role in tumor initiation and progression, and is created by the complex relationship between tumor cells and their surrounding tissues consisting of extracellular matrices, extracellular molecules, and host cells.[1-7] Knowledge of the complicated interplay within these niches however, is still limited. In particular, the exact mechanism of how the host cells that comprise normal stroma are altered during tumor progression and how they reciprocally influence tumor cells during tumorigenesis is poorly understood. By addressing these fundamental issues, the development of therapeutic strategies targeted at specific interactions occurring between the tumor and its microenvironment is ultimately envisaged.

Given that the head and neck region is an environment challenged by a large variety of insults, including pathogens, foods, and chemicals, the aforementioned relationship between cancer cells and inflammatory stroma might be of particular importance for malignancies arising there. Head and neck cancers, over 90% of which are squamous cell carcinomas (SCCs),[8] represent approximately 6% of all new cancers in the United States,[9] and consistently rank as one of the top ten cancers worldwide.[10] More worrying is that the incidence of head and neck cancer appears to be increasing in many parts of the world.[11-14] Head and neck squamous cell carcinoma (HNSCC) is characterized by a high degree of local invasiveness and a high rate of metastasis to the cervical lymph nodes.[15] Survival of patients with HNSCC has not improved in the last 40 years, despite recent advances in surgical procedures and the availability of new chemotherapeutic agents. In addition, surgical treatment results in significant functional and cosmetic defects; therefore, it is important to develop conservative therapeutics, whereupon identification of markers for HNSCC aggressiveness would be worthwhile to decide the most suitable treatment for each patient from therapeutic options.[16]

As with other cancers, most of the head and neck cancer deaths are accounted for by local invasion and distant metastasis. The landmark of carcinoma progression during the invasive and

metastatic phase is epithelial cell plasticity and dedifferentiation, which is similar to epithelial-mesenchymal transition (EMT) that occurs during embryonic development. EMT is the process that cells undergo to switch from a polarized, epithelial phenotype to a motile mesenchymal phenotype.[17-20] Loss of epithelial cell polarity and acquisition of motility results from the disappearance of cell junction adherence molecules, reorganization of cytoskeleton, and redistribution of organelles.[21, 22] Uncovering the mechanism for and identifying the marker of EMT would be strategies to predict tumor progression and possibly develop therapeutic intervention. However, this is complicated by the diversity of molecular mechanisms contributing to the plasticity of epithelial cells in different tissues,[21] especially in cancer tissues *in vivo*.

We have previously reported that parathyroid hormone-related protein (PTHrP) promotes malignant conversion of head and neck cancers in a paracrine or autocrine manner.[23] This finding raises the possibility that PTHrP induces the expression of receptor activator of NF-κB ligand (RANKL), a member of the TNF family, in a manner analogous to osteoblasts.[24-26] Here, we report that RANKL is preferentially expressed in poorly differentiated HNSCC, and plays a critical role in tumor progression *in vivo* in a microenvironment-specific fashion. By utilizing RANKL-expressing cancer cells, RANKL expression is revealed to induce poorly differentiated histology, epithelial mesenchymal transition, and tumor angiogenesis, presumably in a VEGF-independent manner. In view of the fact that tumors cannot exist outside of their respective microenvironments, these findings highlight RANKL and its downstream signaling as an *in vivo* specific marker of tumor progression and an attractive therapeutic target in HNSCC.

Materials and Methods

Cell Culture

Human head and neck squamous cell carcinoma (HNSCC) cell lines HSC-2 (JCRB0622), HSC-3 (JCRB0623), HSC-4 (JCRB0624), SAS (JCRB0260), and Ca9-22 (JCRB0625) were obtained from the Japanese Collection of Research Bioresources (JCRB) cell bank (Osaka, Japan). Human

gingival fibroblasts (HGF, CRL-1740) and murine leukemic monocytes/macrophage cell line RAW264.7 cells (TIB-71) were purchased from American Type Culture Collection (ATCC, Manassas, VA). Cells used in this study, except for RAW 264.7 cells, were maintained in Dulbecco's modified Eagles medium (DMEM; Sigma, St. Louis, MO) supplemented with 10% fetal bovine serum (FBS; complete DMEM) at 37°C under a humidified atmosphere containing 5% CO_2. RAW 264.7 cells were maintained in RPMI 1640 medium supplemented with 10% FBS. Human umbilical vein endothelial cells (HUVECs) were purchased from Lonza (Walkersville, MD) and maintained in complete endothelial basal medium (EBM-2, Lonza).

Antibodies and Reagents

Antibodies to RANKL, TCF8, and β-actin were obtained from Santa Cruz Biotechnology (Santa Cruz, CA). Anti-Flag (M2) and anti-E- or N-cadherin antibodies were from Stratagene (La Jolla, CA) and BD Biosciences Pharmingen (San Diego, CA), respectively. In immunohistochemical analysis, additional monoclonal antibodies against E-cadherin (Zymed/Invitrogen, Carlsbad, CA) and N-cadherin (Takara Bio Inc., Otsu, Japan) were utilized. Anti-CD31 and Slug antibodies were from Abcam (Cambridge, UK) and Cell Signaling Technology (Danvers, MA), respectively. Human recombinant osteoprotegerin (OPG, TNFRSF11B)/Fc chimera, an anti-VEGF antibody, and a human VEGF ELISA kit were from R&D SYSTEMS (Minneapolis, MN). Human recombinant RANKL and VEGF were purchased from PeproTech (Rocky Hill, NJ).

Ethics

Tumor tissues from patients who had signed a written informed consent document were used for this study. We also obtained approval from the Institutional Review Board of Hokkaido University Hospital.

RNA Isolation and RT-PCR

Total RNA isolation, first strand cDNA synthesis, and PCR were performed as described previously.[27] The sequences for primers used are denoted in Table 1. PCR was performed using a

thermal cycler as follows: denaturation at 94°C for 30 sec, annealing at 58 and 60°C (for RANKL and GAPDH, respectively) for 30 sec, extension at 72°C for 30 sec, followed by a final incubation at 72°C for 10 min. PCR products were subjected to 1% agarose gel electrophoresis, stained with ethidium bromide, and detected using an image analyzer (ATTO, Tokyo, Japan). Quantitative real-time RT-PCR was performed as described[28] using a StepOne real-time PCR system (Applied Biosystems, Foster City, CA) and the same primers as for the conventional RT-PCR, except those for RANKL (Table 1). Data are normalized by the expression level of GAPDH and expressed as fold increase compared to control indicated in the Figure Legends. Of note, all primers except those for mouse VEGF were designed to amplify human mRNAs.

Pathological Examination and Immunohistochemistry

Formalin-fixed, paraffin-embedded tissue sections (4 μm) of head and neck cancer samples were deparaffinized and rehydrated. These deparaffinized sections were stained with hematoxylin and eosin (HE) by the conventional method. Histological classifications were performed by two pathologists independently, according to two common criteria for SCC: one is grades of differentiation, in which histological differentiation was divided into well- (stratified squamous cell nest≥ 50%), poorly (< 5%), and moderately (the rest) differen tiated SCCs; another is the Yamamoto-Kohama's classification, a histological grading of mode of invasion, in which tumor tissues were categorized into 4 groups (1, well-defined borderline; 2, cords, less marked borderline; 3, groups of cells, no distinct border line; 4, Diffuse invasion).[29]

The sections were also immersed in 10 mM citrate buffer (pH 6.0) and heated in a pressure cooker for antigen retrieval, followed by incubation in 3% H_2O_2 peroxidase blocking solution. For RANKL staining, the specimens were treated with 100 mM glycine solution (pH 3.0) for 20 min before the blocking step. After incubation in 1% bovine serum albumin (BSA) blocking solution for 30 min, the sections were then incubated with a primary antibody for RANKL (FL-317), E-cadherin (4A2 C7), N-cadherin (M142) or CD31 (ab28364) for 1 h, biotinylated secondary antibody, avidin/biotin C solution, and peroxidase substrate solution. Microscopic

observation was performed after counterstaining with hematoxylin.

To semi-quantify RANKL expression, staining intensity, evaluated by two pathologists independently, was categorized into 5 groups: 1, no detectable immunoreactivity; 2, weak staining; 3, moderate staining; 4, moderate to intense staining; 5, intense staining. The staining intensity of the surrounding tissue was used as a basal-level reference.

Immunoblotting

Cells were lysed in a solution containing 10 mM Tris-HCl (pH 7.4), 5 mM EDTA, 150 mM NaCl, 10% glycerol, 1% Triton X-100, 1% sodium deoxycholate, 0.1% SDS, 50 mM NaF, 1 mM Na_3VO_4, and complete (EDTA-free) protease inhibitor (Roche, Indianapolis, IN) for 20 min on ice and clarified by microcentrifugation at 14,000 rpm for 10 min at 4°C. Supernatants were subjected to SDS-PAGE, and separated proteins were transferred to polyvinylidene difluoride membranes (Bio-Rad, Hercules, CA). The membranes were incubated with primary antibodies, followed by horseradish peroxidase-labeled secondary antibodies. Signals were developed using ECL Western Blotting Detection Reagent (GE Healthcare, UK) and detected using an LAS-1000UVmini image analyzer (FUJIFILM, Tokyo, Japan).

Establishment of RANKL-Expressing Cancer Cells

Full-length cDNA for human RANKL was kindly provided from Dr. Takayanagi (Tokyo Medical and Dental University, Tokyo, Japan) and subcloned into the *Xho*I and *Not*I site of a pCXN2-Flag expression vector.[30]

HSC-3 cells were then transfected with pCXN2-Flag-RANKL or its control vector without RANKL expression, with the use of Fugene HD reagent (Roche). Starting at two days after transfection, the cells were cultured in complete DMEM containing 0.5 mg/ml G418 (Sigma). After 10 days, the resistant cells were together harvested and cultured for further 7 days. Stably transfected cells, in which RANKL expression was examined by RT-PCR and immunoblotting analyses, were maintained in culture media supplemented with 0.2 mg/ml G418.

In Vivo *Tumor Formation in Nude Mice*

Mice breeding and experiments were approved by the institutional animal care and experiment committee of Hokkaido University. Nude mice (BALB/cA Jc1 nu/nu) were injected with HNSCC cells and control or RANKL-expressing HSC-3 cells in their muscles in masseter or hindlimb regions. Of note, the former region is one of the established sites for an oral cancer orthotopic model,[31-33] whereas the latter is chosen as a muscle existing far from the oral tissue. Total RNA from developed tumors was isolated using the RNeasy mini kit and analyzed as described in the section of RNA isolation and RT-PCR. Proteins were extracted through lysis as described in the immunoblotting section. Formalin-fixed paraffin sections were also prepared and stained with hematoxylin and eosin (HE) by conventional methods.

Osteoclastogenesis

Raw 264.7 cells and RANKL-expressing or control HSC-3 cells were co-cultured for 6 d. The cells were fixed with 8% glutaraldehyde and subjected to tartrate-resistant acid phosphatase (TRAP) staining as described previously.[33] As a positive control for TRAP staining, Raw264.7 cells were also cultured in the presence of 100 ng/ml RANKL for 4 d. RAW264.7 cells were cultured in a 96-well plate. After 24 h, cancer cells stained with Hoechest33342 (Molecular Probes) were added on a RAW264.7 cell monolayer, and allowed to adhere for 30 min. The medium was then removed, and the adherent cells were quantified by measuring the fluorescence at 480 nm with an excitation wavelength of 375 nm.

Cell Proliferation and Wound-Healing Assays

The cell proliferation was measured by counting every other day for 8 days after 5×10^4 cell plating. A wound-healing assay was performed as described previously[23]. Briefly, confluent cells were wounded by scraping with a P200 pipette tip. Cell movements were then observed by phase-contrast microscopy.

Three Dimensional (3D) Culture and Colony Formation in Gels

Collagen gel and Matrigel cultures were essentially performed as described previously[34] with some modifications according to the manufacturer's protocol. Briefly, cells (2×10^4) were resuspended in 0.5 ml complete DMEM containing 0.3% collagen (type I-A, Nitta Gelatin, Osaka, Japan), and plated on a 12-well dish. After the collagen solution had gelled, 1 ml complete DMEM was added to each well and changed every 7 days. Alternatively, the cells were resuspended in 0.8 ml Matrigel (BD-Discovery Labware, Bedford, MA), and plated on a 24-well dish. After the Matrigel had gelled, 0.5 ml complete DMEM was added to each well and changed every 7 days. After 21 days, colonies were photographed.

Endothelial Cell Migration Assay

The chemotaxis assay was performed using 24-well Cell Culture Inserts with 8.0-μm pores (Nunc, Kamstrupvej, Denmark), as described previously.[28] Conditioned media obtained were added as a chemoattractant into the lower chamber, and HUVECs (1.5×10^4) were seeded in the upper chamber. In some experiments, OPG (100 ng/ml) or an anti-VEGF antibody (1 μg/ml) was added to the media. Recombinant human VEGF (10 ng/ml) was also used as a control. After 24 h incubation at 37°C, transferred HUVECs to the lower surface of filters were fixed and stained by 0.2% crystal violet, and the cell number in randomly selected fields was counted. Levels of secreted VEGF in conditioned media were analyzed by enzyme-linked immunosorbent assay (ELISA) according to the manufacturer's recommendation.

Statistical Analysis

All data, unless otherwise specified, are expressed as the mean ± standard deviation (S.D.), subjected to one-way analysis of variance, followed by comparison using a Student's *t*-test, a Mann-Whitney U test, or a Spearman's test to evaluate the difference between the samples. A P value less than 0.05 was considered significant in each test, is represented by an asterisk over the error bars in the figures, and is described in the figure legends.

Results

RANKL Expression in Human Head and Neck Cancer Tissues and Cell Lines

To explore the possible implication of RANKL in HNSCC progression, we first examined the expression of RANKL mRNA by quantitative RT-PCR in 20 human HNSCC samples, including those in the tongue and the gingiva. In all cases, high expression (from 6 to 123-fold) is observed compared to human gingival fibroblast, HGF (Figure 1A). Next, to clarify the relationship between RANKL expression and HNSCC progression, HNSCC samples were categorized into various groups that are based on difference in clinical staging or histological differentiation, and RANKL expression levels were compared across the groups using non-parametric analyses. The expression level of RANKL was positively correlated with the histological grade of differentiation (Figure 1B), but not with tumor-node-metastasis (TNM) staging (rank correlation coefficient: $\rho = 0.0264$, $P = 0.497$). Because factors related to TNM can be affected by the phase when the patients are diagnosed, this result does not rule out the possibility that RANKL is implicated in progression and biological malignancies of HNSCC. Indeed, when we utilized the Yamamoto-Kohama classification, a criterion based on histological architecture and mode of invasion,[29] strikingly high expression was observed in a YK-4 group (diffuse invasive type; Figure 1C).

When cases were available for histological examination (n = 16), immunohistochemical analysis was also performed to further evaluate the role of the RANKL protein in HNSCC malignancy, and revealed that poorly differentiated SCC (YK4), in which atypical cancer cells diffusely invaded into surrounding tissues, expressed abundant RANKL proteins (Figure 1D, left panels). Meanwhile, the level was low in well-differentiated SCC (YK-3), in which tumor cells showed expanded growth with obvious keratinization (Figure 1D, right panels). Statistical analyses also elucidated that RANKL expression was correlated with the histological grade of differentiation and mode of invasion (Figure 1, E and F). Thus, the expression level of RANKL is intimately associated with the grade of histological differentiation of HNSCC. Nevertheless, to

our surprise, none of the tested HNSCC cell lines, namely, HSC-2–4, SAS, and Ca9-22, displayed such abundant RANKL expression as that observed *in vivo*, albeit the expression in these cell lines, except for HSC-2, is higher than that in HGF (~3.2-fold) (see also Figure 1A). In particular, although the HSC-2, HSC-3, and SAS cell lines are established from moderately to poorly differentiated SCC with aggressive invasiveness, and in fact displayed similar characteristics when the cells were inoculated into mice oral tissue (see below), the RANKL expression level in these cell lines might be repressed under culture conditions.

Environment-Dependent Expression of RANKL

We thus hypothesized that repressed RANKL expression under culture conditions is due to a lack of environmental cues that are required for the maintenance of its expression. To test this possibility, HSC-3 cells were inoculated into the masseter muscles of mice (one of the most established sites for a head and neck cancer orthotopic model),[31-33] and the amount of RANKL mRNA was analyzed by RT-PCR using a primer set specific for human RANKL. As expected, RANKL expression in all tumor tissues tested (n = 3) was dramatically augmented (Figure 2A, upper panels, lane 2–4; Figure 2B, middle panel, right two columns) compared to that in cultured cells (Figure 2A, lane 1; Figure 2B, middle panel, left column). RANKL protein was also upregulated *in vivo* compared with culture conditions (Figure 2A, lower panels). Moreover, when all other available HNSCC cell lines, namely HSC-2, HSC-4, SAS, and Ca9-22, were inoculated into mice masseter regions, HSC-2 and SAS could form obvious tumors, and RANKL upregulation was observed in these tumors (Figure 2B). Histological examination revealed that HSC-3 and SAS displayed poorly differentiated SCC, while HSC-2 showed moderate differentiation (Figure 2C), in accordance with our clinicopathological findings that RANKL expression correlated with histological grade and invasion mode (see Figure 1). In addition, consistent with the established role for RANKL in bone resorption,[35-37] we could also observe bone destructive lesions accompanied by the accumulation of tartrate-resistant acid phosphatase (TRAP)-positive, mature osteoclasts (Figure 2D), affirming that inoculated HNSCCs expressed

functional RANKL protein.

To assess the contribution of the oral environment to RANKL expression and subsequent tumor formation, HSC-3 cells were also injected into the muscle of hindlimbs, which was selected in analogy to the orthotopic site (intramuscular) and by the distance from the head and neck region. As shown in Figure 2, E and F, tumors formed in the hindlimbs (H) were significantly smaller than those in the masseter region (M). In parallel with tumor weight, RANKL could be detected in the masseter region tumors (Figure 2G; M1 and M2), but not in the hindlimb ones (Figure 2G; H1 and H2) at both mRNA and protein levels. Essentially similar results were obtained when HSC-2 and SAS cells were used (data not shown). Thus, RANKL expression requires the orthotopic environment and correlates with tumor formation ability.

RANKL Expression Accelerates Tumor Formation

Because none of the HNSCC cell lines expressed RANKL plentifully, compared to the *in vivo* condition, we established HNSCC cell lines that stably express RANKL, in order to further confirm the role for RANKL in HNSCC tumor formation. Of the cell lines that were able to form tumors in the masseter region (see Figure 2), we utilized HSC-3 cells, which display poorly differentiated, invasive SCC uniformly without apparent necrosis (see Figure 2C). Among several established cell lines, two control vector-transfected cell lines (C1 and C2), and two RANKL-expressing cell lines (R1 and R2) were used in the following experiments. These R1 and R2 cells appeared to express sufficient amounts of RANKL mRNA and RANKL protein (Figure 3A). Moreover, in view of induction of mature osteoclasts from RAW264.7 cells (Figure 3B, arrow heads) and adhesiveness to a RAW264.7 cell monolayer (Figures 3, C and D), the expressed RANKL was apparently functional. Under these conditions, C1 and R2 cells were injected into the mouse hindlimbs in which both RANKL expression and tumor formation were abolished in parental HNSCC lines (see Figure 2, E–G). It is to our surprise that RANKL-expressing cells achieved efficient tumor formation in the hindlimbs (Figure 4, A and B), whereas C1 cells, in which RANKL expression was not observed even after the inoculation

(Figure 4, C and D), failed to form sizable tumors (Figure 4, A and B), similar to parental cells (see also Figure 2E). These results together demonstrate that RANKL expression, which ordinarily depends on the head and neck environment, possesses the potential of inducing HNSCC formation.

Given that RANKL expression positively correlated with histological grading of differentiation in human HNSCC samples (see Figure 1, B–F), we examined the histology of the tumor formed by control and RANKL-expressing cells. By HE staining, it was revealed that RANKL-expressing, hindlimb-injected tumors exhibited more poorly differentiated and invasive characters than control tumors (Figure 4E), consistent with the results observed in human specimens (see Figure 1, B–F). In these tumors, RANKL expression was detected at the protein level by immunohistochemistry (Figure 4F). We further performed immunohistochemical analysis to visualize the localization of the cell-cell adhesion molecule E-cadherin, one of the most important hallmarks of epithelial cells. Loss of E-cadherin localization from the cell-to-cell contact sites was specifically observed in tumors formed by RANKL-expressing cells (Figure 4G, lower panel), whereas control tumors displayed typical E-cadherin localization at the cell-to-cell borders (Figure 4G, upper panel). Moreover, in response to E-cadherin disappearance from the plasma membrane, intense staining for N-cadherin was observed in the tumor cell cytoplasm in RANKL-expressing tumors (Figure 4H). These findings raise the possibility that RANKL promotes loss of epithelial character, that is epithelial mesenchymal transition (EMT), a fundamental process in tumor development and progression.[38]

RANKL Induced Malignant Phenotypes in an In Vivo*-Specific Manner*

To test whether RANKL-expressing tumors in fact underwent EMT, we evaluated the expression levels of E-cadherin, N-cadherin, and several transcription factors implicated in EMT.[21] However, we could note no differences in their expression *in vitro* (data not shown). Moreover, notwithstanding the dramatic increment in tumor formation of RANKL-expressing cells in the hindlimbs, *in vitro* proliferation of R2 cells was substantially slower than that of C1 cells (Figure

5A). In addition, there is no significant difference in *in vitro* motility (Figure 5B) or invasiveness (data not shown) between these two cell lines.

Hence, we assumed that RANKL function differs between *in vivo* and *in vitro* conditions, i.e. RANKL can promote tumor growth and EMT in an *in vivo*-specific manner. Indeed, expression of E-cadherin was significantly decreased in RANKL-expressing tumor cells at both protein and mRNA levels, as measured by Western blotting (Figure 6A) and quantitative RT-PCR (Figure 6B), respectively. Accordingly, N-cadherin expression was dramatically upregulated in tumor tissues expressing RANKL (Figure 6, A and B). An increase in N-cadherin expression was also observed in tumors arising from HNSCCs inoculated to the mouse masseter region (Figure 6C). Therefore, these results confirmed that cadherin switching from E-cadherin to N-cadherin accrued in tumors expressing RANKL. We further examined the levels of several mRNA transcripts for transcription factors implicated in inducing EMT, including Slug, Snail, Twist, and TCF8 (alternatively known as ZEB1 or δEF1). Of these, Slug and TCF8, but not Snail and Twist, were upregulated at both mRNA and protein levels in RANKL-expressing tumors (Figure 6, D and E). Furthermore, when we inoculated cells in gels and observed the morphology of formed colonies, RANKL-expressing cells efficiently formed colonies with a higher invasive character (epithelial branching, an EMT-dependent event)[39] than control cells in both a collagen gel and Matrigel (Figure 6F), meaning that RANKL promotes EMT and enhances invasiveness in a 3D environment.

Tumor angiogenesis induced by RANKL

It is well established that tumor angiogenesis is critical not only for tumor growth but also its malignant properties, including invasiveness. Because RANKL expressing tumors were grossly rich in blood vessels (Figure 7A, right panel), we thus evaluated another function of RANKL in promoting angiogenesis. Immunohistochemical analysis using an antibody against CD31, a well-established marker for endothelial cells, revealed that RANKL-expressing tumors harbor significantly more abundant tumor microvessels than control tumors (Figure 7, B and C). It is

reported that endothelial cells are activated in response to RANKL via its cognate receptor RANK;[40] this encouraged us to examine whether RANKL-expressing cells are capable of mobilizing endothelial cells. To do this, we utilized conditioned media from C1 and R2 cells as chemoattractants for human umbilical vein endothelial cells (HUVECs) and evaluated their migration ability. The number of migrating HUVECs toward culture medium of C1 cells was marginally upregulated compared to that toward control DMEM. In contrast, conditioned medium of R2 cells substantially facilitated HUVEC migration, which was reverted in the presence of osteoprotegerin (OPG), a RANKL decoy receptor that inhibits RANK-RANKL signaling (Figure 7D). It is noteworthy that an equivalent level of vascular endothelial growth factor (VEGF) was secreted in media of both C1 and R2 cells (Figure 7E). In addition, expression levels of human and murine VEGF were not altered, regardless of RANKL expression and whether cell growth conditions were *in vivo* or *in vitro*, as measured by RT-PCR using primers specific for respective species (Figure 7F). Moreover, the HNSCC- or RANKL-dependent HUVEC migration could not be hampered by an anti-VEGF antibody, which at a same concentration almost completely inhibited the migration induced by VEGF (Figure 7G) These results together demonstrate that expressed RANKL promotes tumor angiogenesis in a manner independent of VEGF.

Discussion

In the present study, we disclose that RANKL expression is specifically detected in the intravital environment, which in turn promotes EMT, tumorigenesis, and angiogenesis of HNSCCs *in vivo*. These observations highlight RANKL as a "bio-functional" marker molecule that should be useful for both diagnosis and therapy of this disease.

One of the most serious clinical concerns accompanying HNSCC is a high potential for local invasion, frequently targeting the adjacent bone, thus requiring radical surgical procedures that put much strain on patients due to the deprivation of fundamental functions, including mastication and vocalization. In the future, after appropriate preclinical and clinical tests, the

recognition of RANKL and its relevant signaling as potential targets for conservative therapy may enable us to hamper tumorigenesis and invasion by cutting the connection between HNSCC and the tumor microenvironment. In addition to the conventional molecular targeted therapy (i.e. small compounds and humanized antibodies), RANKL may constitute a better candidate for cancer immunotherapy. Several tumor antigens such as cancer-testis antigens provide specific targets for cancer cells due to their restricted expression patterns.[41-43] However, in the case that these molecules are not essential for cancer cell survival, the cells can escape the challenge of the immune system by reducing the expression of the antigens. Since the expression of RANKL in response to the microenvironment is critical for HNSCC progression (Figures 2 and 4), it is definitively a possibility that RANKL-RANK signaling might be central to the conservative, multimodal treatment for this disease.

EMT, which is characterized by the loss of epithelial characteristics and the acquisition of mesenchymal phenotypes, is an important event in the progression towards more invasive and metastatic cancerous cells. During EMT, tumor cells upregulate mesenchymal markers such as vimentin and Snail, and downregulate epithelial markers such as E-cadherin.[22] It was previously reported that in SCC cells there is a hierarchy of EMT-regulating transcription factors, in which Snail locates on the vertex, especially in the cells with mesenchymal phenotypes.[44] As in other malignancies, several reports also suggest Snail is a most potent E-cadherin suppressor.[20, 45-49] Most of these studies, however, utilize cultured cell lines and overexpression experiments in their analyses. Moreover, few common carcinoma cell types with a well-defined epithelial phenotype can complete EMT *in vitro*, probably because EMT is very sensitive to culture conditions, including substrates and the presence of serum.[22] Indeed, Onoue *et al*. reported that an SDF-1/CXCR4-dependent morphological change to a fibroblast phenotype is dependent on culture conditions, including serum starvation and low confluence.[15] On the other hand, our results clearly indicate that RANKL-induced EMT observed *in vivo* is accounted for by upregulation of Slug and TCF8, but not Snail and Twist (Figure 6, D and E). Supporting of this view, in cells

obtained from recurrent tumors, TCF8 and SIP1 (ZEB2) overexpression, but not Snail upregulation, were specifically detected, relative to cells from primary tumors.[48] Thus, expression of ZEB family proteins is sufficient to induce EMT *in vivo*. Furthermore, it may be noteworthy that exogenous expression of Snail can further promote loss of E-cadherin even in these ZEB1/2-overexpressing cells. This is consistent with our observation that RANKL-expressing tumors preferentially displayed the upregulation of N-cadherin; rather, E-cadherin repression was not so dramatic (Figure 6B).

Potent tumorigenicity of RANKL-expressing cells reminds us of the properties of cancer stem cells. The invasive feature of these cells appears to be dissimilar to the dormant nature of stem cells. On the other hand, recent accumulating evidence indicates that the EMT, where carcinoma cells ephemerally obtain a highly invasive mesenchymal phenotype, generates cells with stem cell attributes.[50-53] Unfortunately, however, RANKL-expressing cells exhibit no stem cell phenotype (spheroid formation and marker expression) *in vitro* (data not shown). Since the effect of RANKL expression on the promotion of tumor formation and EMT is specific for *in vivo* conditions; the proliferation and motility of these cells were slower than those of control cells (Figure 5), these results cannot rule out the possibility that RANKL-expressing cells might indeed behave like stem cells. In fact, our preliminary experiments revealed that the expression of the hyaluronic acid receptor CD44 that is recently implicated as a cell surface marker of tumor initiating cells of gastrointestinal tract and breast malignancies[54, 55] is specifically observed in *in vivo* conditions, and RANKL can facilitate the shedding of this molecule (T.Y., M.T., and Y.O., unpublished result). Further in-depth studies to clarify the significance of RANKL expression *in vivo* will be required for ablating the tumor initiating cells to prevent the occurrence and recurrence of cancers, which is a current goal among cancer scientists worldwide.

The mechanism by which RANKL is expressed in a manner specific to the microenvironment remains to be addressed. Given the specific character of the head and neck as a gatekeeper of organisms that is always challenged by every pathogen, inflammatory responses

play an indispensable role in HNSCC tumor initiation and progression.[56-60] In fact, genome-wide microarray analyses demonstrate the upregulation of inflammation-associated molecules in this cancer.[61, 62]The head and neck region including the oral cavity is also known as a site abundant in a range of growth factors, which are known to contribute to malignant conversion of HNSCC through activating diverse cancer-related signaling pathways.[23, 54, 55, 63] We thus extended the investigation of RANKL-inducing agents from factors directly implicated in HNSCC malignancy (EGF or PTHrP) to those implicated in EMT (such as TGF-β) as well as inflammatory cytokines (data not shown), but failed to identify it. Because the morphological differences between control and RANKL-expressing cells were observed in colonies formed in a collagen gel and Matrigel (Figure 6F), we thought that the engagement with extracellular matrices is likely to attribute to RANKL induction. Unfortunately, however, no extracellular matrices *per se* could evoke RANKL expression *in vitro* (data not shown). Therefore, we infer that the efficient RANKL expression and the subsequent EMT promotion and tumor progression are orchestrated by the combination of intravital conditions, including growth factors, tumor-associated fibroblasts, extracellular matrices, infiltration of inflammatory cells with the production of cytokines, and cells composing vasculatures.

There are other possibilities that account for the specific observation of RANKL expression *in vivo*. For example, RANKL-expressing cells, which constitute a minor population under culture conditions, may preferentially survive under *in vivo* conditions. Given that the RANKL-expressing cells formed larger colonies than control cells, it is possible that the interaction between the cells and the specific extracellular matrices is consolidated to escape anoikis. Indeed, intimate association between NF-κB, a downstream effector of RANKL and its cognate receptor RANK, and cell adhesion has been described,[64-67] and recently, integrin has been shown to play a role in escaping anoikis.[68] Research addressing this issue should be continued. In either case, we can state that RANKL is an *in vivo*-specific functional marker for HNSCC malignancy.

In summary, we hereby show that RANKL expression was specifically observed *in vivo*, and

expressed RANKL plays a hitherto unidentified role in tumor progression, namely inducing EMT and angiogenesis. It may be noteworthy that aggressiveness of angiogenesis in HNSCC was correlated with RANKL expression level, but not the VEGF level, suggesting that VEGF-independent strategies should be taken into consideration to hamper angiogenesis in HNSCC. The function of RANKL as an EMT inducer was also specific for *in vivo* conditions. In the future, we believe that through our observations and the unveiling of remaining associated issues, the establishment of more rational, potent anti-cancer therapy with consideration of the communication between cancer cells and their respective microenvironment will eventually be accomplished.

Acknowledgements

The authors thank J. Hamada and M. Takahata for the cells, H. Takayanagi for RANKL cDNA, J. Miyazaki for the pCXN2 vector, N. Toyoda for technical assistance, S. Darmanin for critical reading of the manuscript, and members of our laboratories for helpful discussion.

Abbreviations used in this study

DMEM, Dulbecco's modified Eagles medium; EBM, endothelial basal medium; EGF, epidermal growth factor; EMT, epithelial mesenchymal transition; FBS, fetal bovine serum; HGF, human gingival fibroblast; HNSCC, head and neck squamous cell carcinoma; HUVEC, Human umbilical vein endothelial cell; OPG, osteoprotegerin; PTHrP, parathyroid hormone-related protein; RANKL, receptor activator of nuclear factor κB ligand; SCC, squamous cell carcinoma; TGF-β, transforming growth factor-β; TRAP, tartrate-resistant acid phosphatase; VEGF, vascular endothelial growth factor; YK, Yamamoto-Kohama

References

1. Albini A, Sporn MB: The tumour microenvironment as a target for chemoprevention, Nat Rev Cancer 2007, 7:139-147

2. Joyce JA: Therapeutic targeting of the tumor microenvironment, Cancer Cell 2005, 7:513-520

3. Joyce JA, Pollard JW: Microenvironmental regulation of metastasis, Nat Rev Cancer 2008, 9:239-252

4. Liotta LA, Kohn EC: The microenvironment of the tumour-host interface, Nature 2001, 411:375-379

5. Massague J: TGFbeta in Cancer, Cell 2008, 134:215-230

6. Orimo A, Weinberg RA: Stromal fibroblasts in cancer: a novel tumor-promoting cell type, Cell Cycle 2006, 5:1597-1601

7. Polyak K, Haviv I, Campbell IG: Co-evolution of tumor cells and their microenvironment, Trends Genet 2009, 25:30-38

8. Chen AY, Myers JN: Cancer of the oral cavity, Dis Mon 2001, 47:275-361

9. Whiteside ST, Israel A: I kappa B proteins: structure, function and regulation, Semin Cancer Biol 1997, 8:75-82

10. Reichart PA: Identification of risk groups for oral precancer and cancer and preventive measures, Clin Oral Investig 2001, 5:207-213

11. Conway DI, Stockton DL, Warnakulasuriya KA, Ogden G, Macpherson LM: Incidence of oral and oropharyngeal cancer in United Kingdom (1990-1999) -- recent trends and regional variation, Oral Oncol 2006, 42:586-592

12. Llewellyn CD, Linklater K, Bell J, Johnson NW, Warnakulasuriya S: An analysis of risk factors for oral cancer in young people: a case-control study, Oral Oncol 2004, 40:304-313

13. Popovtzer A, Shpitzer T, Bahar G, Marshak G, Ulanovski D, Feinmesser R: Squamous cell carcinoma of the oral tongue in young patients, Laryngoscope 2004, 114:915-917

14. Shiboski CH, Schmidt BL, Jordan RC: Tongue and tonsil carcinoma: increasing trends in the U.S. population ages 20-44 years, Cancer 2005, 103:1843-1849

15. Onoue T, Uchida D, Begum NM, Tomizuka Y, Yoshida H, Sato M: Epithelial-mesenchymal transition induced by the stromal cell-derived factor-1/CXCR4 system in oral squamous cell carcinoma cells, Int J Oncol 2006, 29:1133-1138

16. Chang JY, Wright JM, Svoboda KK: Signal transduction pathways involved in epithelial-mesenchymal transition in oral cancer compared with other cancers, Cells Tissues Organs 2007, 185:40-47

17. Hay ED: An overview of epithelio-mesenchymal transformation, Acta Anat (Basel) 1995, 154:8-20

18. Kalluri R, Weinberg RA: The basics of epithelial-mesenchymal transition, J Clin Invest 2009, 119:1420-1428

19. Thiery JP: Epithelial-mesenchymal transitions in development and pathologies, Curr Opin Cell Biol 2003, 15:740-746

20. Thiery JP: Epithelial-mesenchymal transitions in tumour progression, Nat Rev Cancer 2002, 2:442-454

21. Gotzmann J, Mikula M, Eger A, Schulte-Hermann R, Foisner R, Beug H, Mikulits W: Molecular aspects of epithelial cell plasticity: implications for local tumor invasion and metastasis, Mutat Res 2004, 566:9-20

22. Thiery JP, Sleeman JP: Complex networks orchestrate epithelial-mesenchymal transitions, Nat Rev Mol Cell Biol 2006, 7:131-142

23. Yamada T, Tsuda M, Ohba Y, Kawaguchi H, Totsuka Y, Shindoh M: PTHrP promotes malignancy of human oral cancer cell downstream of the EGFR signaling, Biochem Biophys Res Commun 2008, 368:575-581

24. Leibbrandt A, Penninger JM: RANK/RANKL: regulators of immune responses and bone physiology, Ann NY Acad Sci 2008, 1143:123-150

25. Mundy GR: Metastasis to bone: causes, consequences and therapeutic opportunities, Nat Rev Cancer 2002, 2:584-593

26. Roodman GD: Mechanisms of bone metastasis, N Engl J Med 2004, 350:1655-1664

27. Inuzuka T, Tsuda M, Kawaguchi H, Ohba Y: Transcription factor 8 activates R-Ras to regulate angiogenesis, Biochem Biophys Res Commun 2009, 379:510-513

28. Inuzuka T, Tsuda M, Tanaka S, Kawaguchi H, Higashi Y, Ohba Y: Integral role of transcription factor 8 in the negative regulation of tumor angiogenesis, Cancer Res 2009, 69:1678-1684

29. Yamamoto E, Kohama G, Sunakawa H, Iwai M, Hiratsuka H: Mode of invasion, bleomycin sensitivity, and clinical course in squamous cell carcinoma of the oral cavity, Cancer 1983, 51:2175-2180

30. Niwa H, Yamamura K, Miyazaki J: Efficient selection for high-expression transfectants with a novel eukaryotic vector, Gene 1991, 108:193-199

31. Cui N, Nomura T, Noma H, Yokoo K, Takagi R, Hashimoto S, Okamoto M, Sato M, Yu G, Guo C, Shibahala T: Effect of YM529 on a model of mandibular invasion by oral squamous cell carcinoma in mice, Clin Cancer Res 2005, 11:2713-2719

32. Nomura T, Shibahara T, Katakura A, Matsubara S, Takano N: Establishment of a murine model of bone invasion by oral squamous cell carcinoma, Oral Oncol 2007, 43:257-262

33. Suda T, Jimi E, Nakamura I, Takahashi N: Role of 1 alpha,25-dihydroxyvitamin D3 in osteoclast differentiation and function, Methods Enzymol 1997, 282:223-235

34. Montesano R, Schaller G, Orci L: Induction of epithelial tubular morphogenesis in vitro by fibroblast-derived soluble factors, Cell 1991, 66:697-711

35. Lacey DL, Timms E, Tan HL, Kelley MJ, Dunstan CR, Burgess T, Elliott R, Colombero A, Elliott G, Scully S, Hsu H, Sullivan J, Hawkins N, Davy E, Capparelli C, Eli A, Qian YX, Kaufman S, Sarosi I, Shalhoub V, Senaldi G, Guo J, Delaney J, Boyle WJ: Osteoprotegerin ligand is a cytokine that regulates osteoclast differentiation and activation, Cell 1998, 93:165-176

36. Takahashi N, Udagawa N, Suda T: A new member of tumor necrosis factor ligand family, ODF/OPGL/TRANCE/RANKL, regulates osteoclast differentiation and function, Biochem Biophys Res Commun 1999, 256:449-455

37. Yasuda H, Shima N, Nakagawa N, Yamaguchi K, Kinosaki M, Mochizuki S, Tomoyasu A, Yano K, Goto M, Murakami A, Tsuda E, Morinaga T, Higashio K, Udagawa N, Takahashi N, Suda T: Osteoclast differentiation factor is a ligand for osteoprotegerin/osteoclastogenesis-inhibitory factor and is identical to TRANCE/RANKL, Proc Natl Acad Sci USA 1998, 95:3597-3602

38. Yang J, Weinberg RA: Epithelial-mesenchymal transition: at the crossroads of development and tumor metastasis, Dev Cell 2008, 14:818-829

39. Shintani Y, Wheelock MJ, Johnson KR: Phosphoinositide-3 kinase-Rac1-c-Jun NH2-terminal kinase signaling mediates collagen I-induced cell scattering and up-regulation of N-cadherin expression in mouse mammary epithelial cells, Mol Biol Cell 2006, 17:2963-2975

40. Kim YM, Lee YM, Kim HS, Kim JD, Choi Y, Kim KW, Lee SY, Kwon YG: TNF-related activation-induced cytokine (TRANCE) induces angiogenesis through the activation of Src and phospholipase C (PLC) in human endothelial cells, J Biol Chem 2002, 277:6799-6805

41. Maio M, Coral S, Fratta E, Altomonte M, Sigalotti L: Epigenetic targets for immune intervention in human malignancies, Oncogene 2003, 22:6484-6488

42. Nicholaou T, Ebert L, Davis ID, Robson N, Klein O, Maraskovsky E, Chen W, Cebon J: Directions in the immune targeting of cancer: lessons learned from the cancer-testis Ag NY-ESO-1, Immunol Cell Biol 2006, 84:303-317

43. Suri A: Cancer testis antigens--their importance in immunotherapy and in the early detection of cancer, Expert Opin Biol Ther 2006, 6:379-389

44. Taki M, Verschueren K, Yokoyama K, Nagayama M, Kamata N: Involvement of Ets-1 transcription factor in inducing matrix metalloproteinase-2 expression by epithelial-mesenchymal transition in human squamous carcinoma cells, Int J Oncol 2006, 28:487-496

45. Batlle E, Sancho E, Franci C, Dominguez D, Monfar M, Baulida J, Garcia De Herreros A: The transcription factor snail is a repressor of E-cadherin gene expression in epithelial tumour cells, Nat Cell Biol 2000, 2:84-89

46. Cano A, Perez-Moreno MA, Rodrigo I, Locascio A, Blanco MJ, del Barrio MG, Portillo F, Nieto MA: The transcription factor snail controls epithelial-mesenchymal transitions by repressing E-cadherin expression, Nat Cell Biol 2000, 2:76-83

47. De Craene B, Gilbert B, Stove C, Bruyneel E, van Roy F, Berx G: The transcription factor snail induces tumor cell invasion through modulation of the epithelial cell differentiation program, Cancer Res 2005, 65:6237-6244

48. Takkunen M, Grenman R, Hukkanen M, Korhonen M, Garcia de Herreros A, Virtanen I: Snail-dependent and -independent epithelial-mesenchymal transition in oral squamous carcinoma cells, J Histochem Cytochem 2006, 54:1263-1275

49. Yokoyama K, Kamata N, Hayashi E, Hoteiya T, Ueda N, Fujimoto R, Nagayama M: Reverse correlation of E-cadherin and snail expression in oral squamous cell carcinoma cells in vitro, Oral Oncol 2001, 37:65-71

50. Hollier BG, Evans K, Mani SA: The epithelial-to-mesenchymal transition and cancer stem cells: a coalition against cancer therapies, J Mammary Gland Biol Neoplasia 2009, 14:29-43

51. Klarmann GJ, Hurt EM, Mathews LA, Zhang X, Duhagon MA, Mistree T, Thomas SB, Farrar WL: Invasive prostate cancer cells are tumor initiating cells that have a stem cell-like genomic signature, Clin Exp Metastasis 2009, 26:433-446

52. Mani SA, Guo W, Liao MJ, Eaton EN, Ayyanan A, Zhou AY, Brooks M, Reinhard F, Zhang CC, Shipitsin M, Campbell LL, Polyak K, Brisken C, Yang J, Weinberg RA: The epithelial-mesenchymal transition generates cells with properties of stem cells, Cell 2008, 133:704-715

53. Morel AP, Lievre M, Thomas C, Hinkal G, Ansieau S, Puisieux A: Generation of breast cancer stem cells through epithelial-mesenchymal transition, PLoS ONE 2008, 3:e2888

54. Nagano O, Saya H: Mechanism and biological significance of CD44 cleavage, Cancer Sci 2004, 95:930-935

55. Ponta H, Sherman L, Herrlich PA: CD44: from adhesion molecules to signalling regulators, Nat Rev Mol Cell Biol 2003, 4:33-45

56. Allen CT, Ricker JL, Chen Z, Van Waes C: Role of activated nuclear factor-kappaB in the pathogenesis and therapy of squamous cell carcinoma of the head and neck, Head Neck 2007, 29:959-971

57. Choi S, Myers JN: Molecular pathogenesis of oral squamous cell carcinoma: implications for therapy, J Dent Res 2008, 87:14-32

58. Ferris RL, Grandis JR: NF-kappaB gene signatures and p53 mutations in head and neck squamous cell carcinoma, Clin Cancer Res 2007, 13:5663-5664

59. Lin DT, Subbaramaiah K, Shah JP, Dannenberg AJ, Boyle JO: Cyclooxygenase-2: a novel molecular target for the prevention and treatment of head and neck cancer, Head Neck 2002, 24:792-799

60. Pries R, Nitsch S, Wollenberg B: Role of cytokines in head and neck squamous cell carcinoma, Expert Rev Anticancer Ther 2006, 6:1195-1203

61. Ginos MA, Page GP, Michalowicz BS, Patel KJ, Volker SE, Pambuccian SE, Ondrey FG, Adams GL, Gaffney PM: Identification of a gene expression signature associated with recurrent disease in squamous cell carcinoma of the head and neck, Cancer Res 2004, 64:55-63

62. Ziober AF, Patel KR, Alawi F, Gimotty P, Weber RS, Feldman MM, Chalian AA, Weinstein GS, Hunt J, Ziober BL: Identification of a gene signature for rapid screening of oral squamous cell carcinoma, Clin Cancer Res 2006, 12:5960-5971

63. Todd R, Wong DT: Epidermal growth factor receptor (EGFR) biology and human oral cancer, Histol Histopathol 1999, 14:491-500

64. Lin TH, Rosales C, Mondal K, Bolen JB, Haskill S, Juliano RL: Integrin-mediated tyrosine phosphorylation and cytokine message induction in monocytic cells. A possible signaling role for the Syk tyrosine kinase, J Biol Chem 1995, 270:16189-16197

65. Narayanan R, Higgins KA, Perez JR, Coleman TA, Rosen CA: Evidence for differential functions of the p50 and p65 subunits of NF-kappa B with a cell adhesion model, Mol Cell Biol 1993, 13:3802-3810

66. Qwarnstrom EE, Ostberg CO, Turk GL, Richardson CA, Bomsztyk K: Fibronectin attachment activates the NF-kappa B p50/p65 heterodimer in fibroblasts and smooth muscle cells, J Biol Chem 1994, 269:30765-30768

67. Sokoloski JA, Sartorelli AC, Rosen CA, Narayanan R: Antisense oligonucleotides to the p65 subunit of NF-kappa B block CD11b expression and alter adhesion properties of differentiated HL-60 granulocytes, Blood 1993, 82:625-632

68. Desgrosellier JS, Barnes LA, Shields DJ, Huang M, Lau SK, Prevost N, Tarin D, Shattil SJ, Cheresh DA: An integrin alpha(v)beta(3)-c-Src oncogenic unit promotes anchorage-independence and tumor progression, Nat Med 2009, 15:1163-1169

Figure Legends

Figure 1. Expression of RANKL in human head and neck cancers. (A) The mRNA levels of RANKL in surgical specimens of human head and neck cancers and head and neck squamous cell carcinoma (HNSCC) cell lines were analyzed by quantitative RT-PCR. Human gingival fibroblasts (HGF) were used as a control. (B) Differentiation of the tumors was determined by two pathologists independently, according to the criterion described in the Materials and Methods, and the expression level of RANKL mRNA in each tumor was plotted. A Spearman's test was used to evaluate the difference between the samples. Rank correlation coefficient: ρ = 0.629, $P < 0.05$. (C) Tissue sections were also analyzed by the pathologists, invasion modes of which were categorized into four groups of the Yamamoto-Kohama's (YK) classification as described in the text. $\rho = 0.876$, $P < 0.01$. (D) Typical histology of tumors with poorly differentiated SCC (left panels) and well-differentiated SCC (right) are shown and the expression levels of RANKL were also analyzed by immunohistochemical staining using anti-RANKL antibody. Bars, 100 μm. (E and F) Staining intensity for RANKL was categorized into 5 groups as described in the Materials and Methods, and plotted against grades of differentiation (E) and invasion mode (F). $\rho = 0.705$; $P < 0.01$ (E); $\rho = 0.756$, $P < 0.01$ (F).

Figure 2. Induction of RANKL expression in the head and neck environment. (A) The human head and neck cancer cells (HSC-3) were inoculated into nude mice and allowed to form tumors. Expression levels of RANKL mRNA (upper panels) and protein (lower panels) were analyzed by semi-quantitative RT-PCR and immunoblotting, respectively. Left lane, cells under culture condition before inoculation to mice were used as a control. (B) The HNSCC lines were inoculated into nude mice and allowed to form tumors. RANKL mRNA levels were evaluated by quantitative RT-PCR. Of the cell lines tested, HSC-2, HSC-3, and SAS cells formed tumors, data of which are shown. Cells under culture conditions before inoculation were used as a control (open column). (C and D) The tissues of tumors formed by cell lines indicated on the top were subjected to histopathological examinations. Photographs of hematoxylin-eosin (HE, C and D)

and tartrate-resistant acid phosphatase (TRAP, D) staining are shown. Bars, 100 μm. (E–G) HSC-3 cells were injected into the masseter (M) or hindlimb (H) region. After 28 days, the tumors formed were photographed (E), and weighed (F; *, $P < 0.05$). Expression levels of RANKL mRNA and protein in the masseter region (M1 and M2) or the hind leg region (H1 and H2) of nude mice were analyzed by semi-quantitative RT-PCR (upper panels) and immunoblotting (lower panels) (G).

Figure 3. Establishment of RANKL-overexpressing cells. (A) Expression of RANKL mRNA and protein were determined by RT-PCR at 36 cycles (upper panels) and immunoblotting using anti-RANKL and anti-Flag antibodies (lower panels), respectively. (B) RAW264.7 cells were co-cultured with C1 (vector-transfected cells) or R2 (RANKL-expressing cells), and stained by TRAP. Bars, 300 μm. (C and D) RAW264.7 cells were pre-cultured in 96-well plates. After 24 h, C1 or R2 cells stained with Hoechst 33342 were added on the RAW cell monolayer and incubated for 30 min. After medium removal, the bound cells were quantified by measuring the fluorescence at an excitation wavelength of 357 nm. * $P < 0.05$ (C). Representative photographs are shown; Bars, 30 μm (D).

Figure 4. Tumor formation in hindlimbs rescued by RANKL expression. (A–D) Control (C1) and RANKL-expressing (R2) cells were injected into muscles of the hind legs, and after 28 days, the tumors were photographed (A) and weighed (B; **, $P < 0.01$). RANKL mRNA in tumors formed by C1 or R2 cells was examined by semi-quantitative (C) and quantitative (D) RT-PCR. (E–H) Histopathology of HNSCC in the presence or absence of RANKL expression. Pathological section from tumors formed by C1 and R2 cells were stained by HE and photographed (E). The sections were also subjected to immunohistochemistry using an anti-RANKL (F), E-cadherin (G), or N-cadherin (H) antibody. Arrows indicate striated muscles. Bars, 100 μm. The upper right image in the bottom of (H) is a magnified photograph of the inset.

Figure 5. The effect of RANKL expression on cell proliferation and motility *in vitro*. (A) The number of C1 and R2 cells were counted every three days and plotted. (B) C1, R1, and R2 cells were cultured on type I collagen-coated plates, allowed to form a cell monolayer, and subjected to a wound-healing assay. Relative wound closure compared to C1 cells is shown.

Figure 6. HNSCC EMT promoted by RANKL. (A and B) Alteration in expression levels of E-cadherin and N-cadherin. Protein and mRNA expression levels of these molecules in tumors formed by C1 and R2 cells were determined by immunoblotting (A) and quantitative RT-PCR (B), respectively. *, $P < 0.01$; **, $P < 0.005$. (C) Expression levels of E-cadherin and N-cadherin mRNA in tumors formed by indicated HNSCCs (see Figure 2B and C) were analyzed by quantitative RT-PCR. (D) Expression of indicated transcription factors implicated in EMT was analyzed by quantitative RT-PCR. *, $P < 0.05$. In (B) and (D), C1 cells were used as a control. (E) Expression of Slug and TCF8 was also analyzed by immunoblotting. (F) C1 and R2 cells were seeded on 12-well plates at a density of 2×10^4 cells per well in 0.3 mg/ml type I collagen-containing DMEM or on 24-well plates in Matrigel, and cultured for 21 days. Representative photographs are shown. Bars, 100 μm.

Figure 7. Tumor angiogenesis induced by RANKL. (A) Photographs of gross examination of tumors shown in Figure 4A. (B) Sections obtained as in Figure 4F-H were stained with an anti-CD31 antibody. Representative photomicrographs are shown. Bars, 0.5 mm. (C) The number of blood vessels visualized by CD31 was counted over three randomly selected high-power fields (HPFs), and the average values are shown with S.D. *, $P < 0.001$. (D) The conditioned medium of C1 or R2 cells was used as a chemoattractant and the HUVEC chemotaxis was examined in the presence or absence of osteoprotegerin (OPG), an inhibitor of RANKL. DMEM was used as a negative control. The numbers of HUVECs migrating to the lower surface of the chambers were counted and are shown as mean ± S.D. *, $P < 0.005$; **, $P < 0.001$. (E) Concentrations of VEGF in conditioned media of C1 and R2 cells were determined by enzyme-linked immunosorbent assay (ELISA). (F) Levels of human and mouse VEGF mRNA were determined

by RT-PCR, using primers specific for each species. RAW264.7 cells were used as a positive control for mouse VEGF. M1, M2, H1, and H2 represent samples of tumors shown in Figure 2G. (G) HUVEC migration toward the indicated conditioned media was examined in the presence (1 μg/ml) or absence of anti-VEGF antibody. DMEM and DMEM containing 10 ng/ml VEGF were used as negative and positive controls, respectively. **, $P < 0.01$; NS, not significant.

Table 1 Primers used for RT-PCR. All primers, unless otherwise specified, are designed to amplify human mRNAs specifically.

Target transcripts	Direction	Sequences
RANKL (conventional)	forward	5'-TGGCACTCACTGCATTTATAGAATT-3'
	reverse	5'-AGTTGAAGATACTCTGTAGCTAGGT-3'
RANKL (real-time)	forward	5'-CGTTGGATCACAGCACATCAG-3'
	reverse	5'-GCTCCTCTTGGCCAGATCTAAC-3'
E-cadherin	forward	5'-TCCATTTCTTGGTCTACGCC-3'
	reverse	5'-CACCTTCAGCCATCCTGTTT-3'
N-cadherin	forward	5'-GTGCCATTAGCCAAGGGAATTCAGC-3'
	reverse	5'-GCGTTCCTGTTCCACTCATAGGAGG-3'
TCF8 (ZEB1; δEF1)	forward	5'-GCTAAGAACTGCTGGGAGGAT-3'
	reverse	5'-TCCTGCTTCATCTGCCTGA-3'
Slug	forward	5'-TGGTTGCTTCAAGGACACAT-3'
	reverse	5'-GTTGCAGTGAGGGCAAGAA-3'
Snail	forward	5'-GCTGCAGGACTCTAATCCAGA-3'
	reverse	5'-ATCTCCGGAGGTGGGATG-3'
Twist	forward	5'-GGCATCACTATGGACTTTCTCTATT-3'
	reverse	5'-GGCCAGTTTGATCCCAGTATT-3'
human VEGF	forward	5'-GGCTCTAGATCGGGCCTCCGAAACCAT-3'
(hVEGF)	reverse	5'-GGCTCTAGAGCGCAGAGTCTCCTCTTC-3'
mouse VEGF	forward	5'-ACATCTTCAAGCCGTCCTGTGTGC-3'
(mVEGF)	reverse	5'-AAATGGCGAATCCAGTCCCACGAG-3'
GAPDH	forward	5'-GAAATCCCATCACCATCTTCCAGG-3'
	reverse	5'-CATGTGGGCCATGAGGTCCACCAC-3'

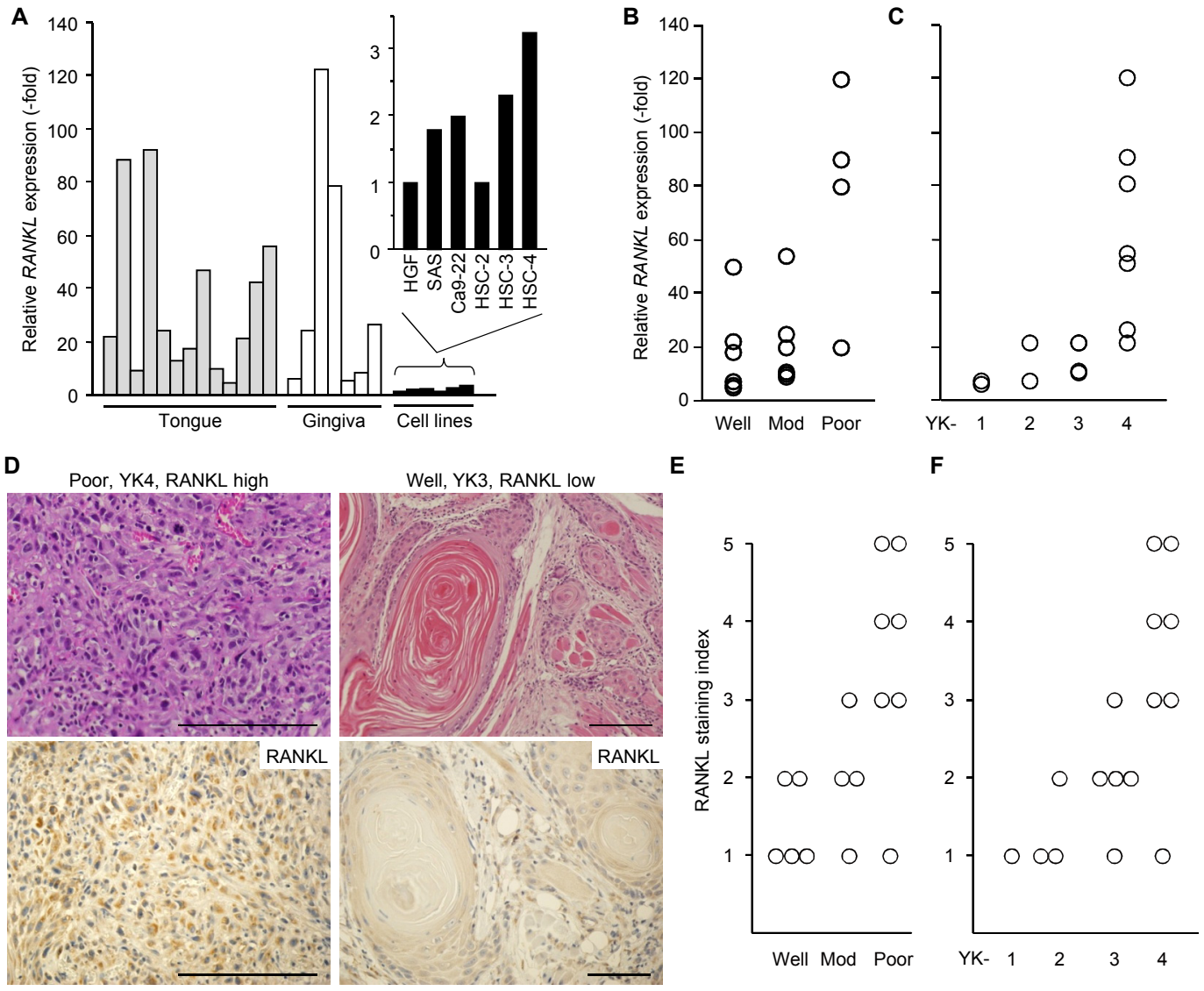

Figure 1 Yamada, T., *et al*.

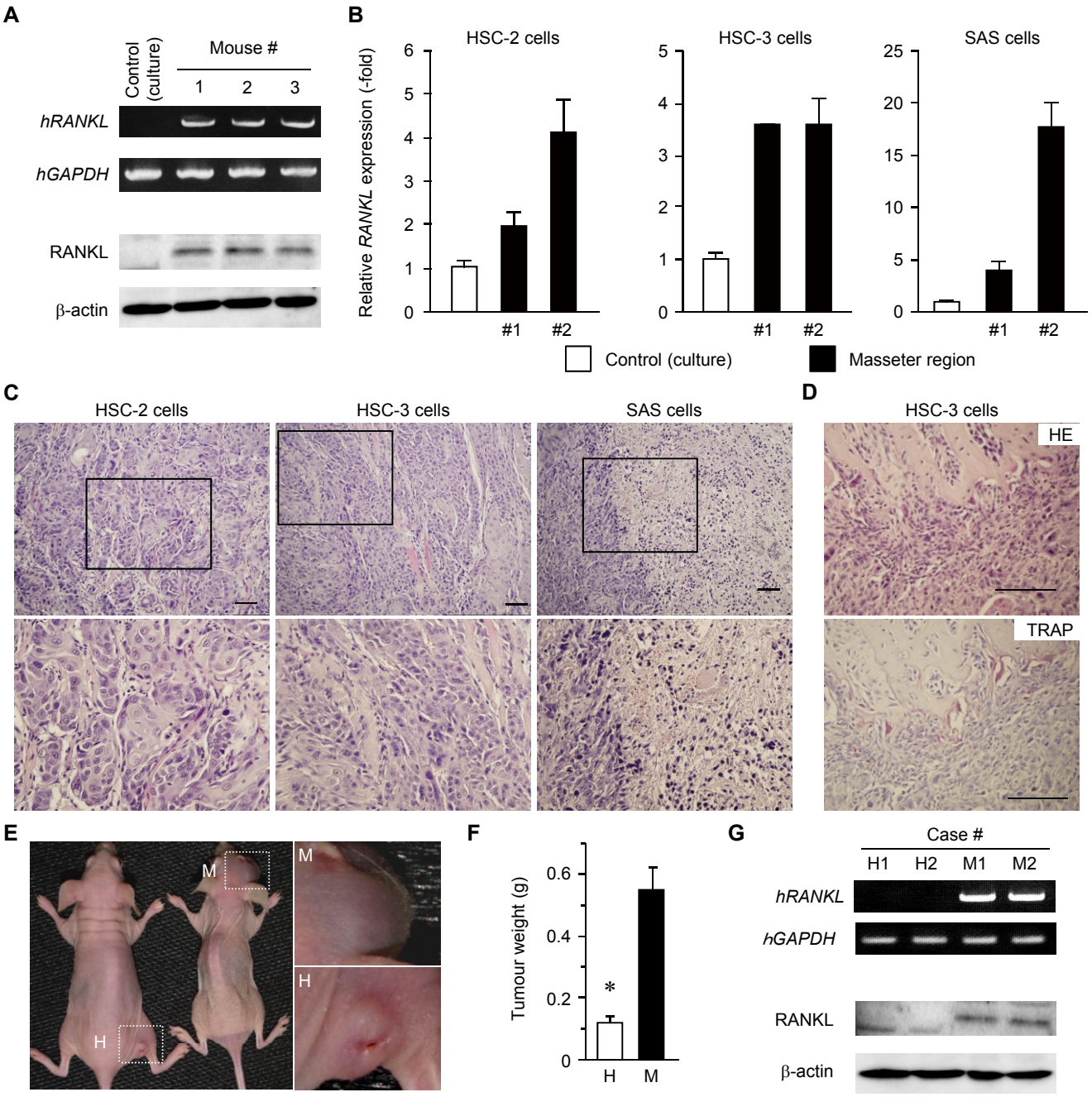

Figure 2 Yamada, T., *et al*.

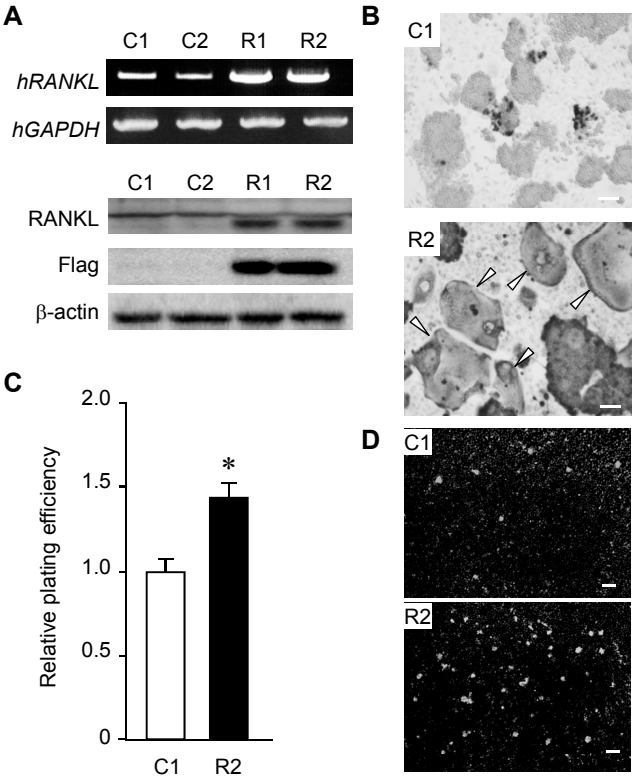

Figure 3 Yamada, T., *et al*.

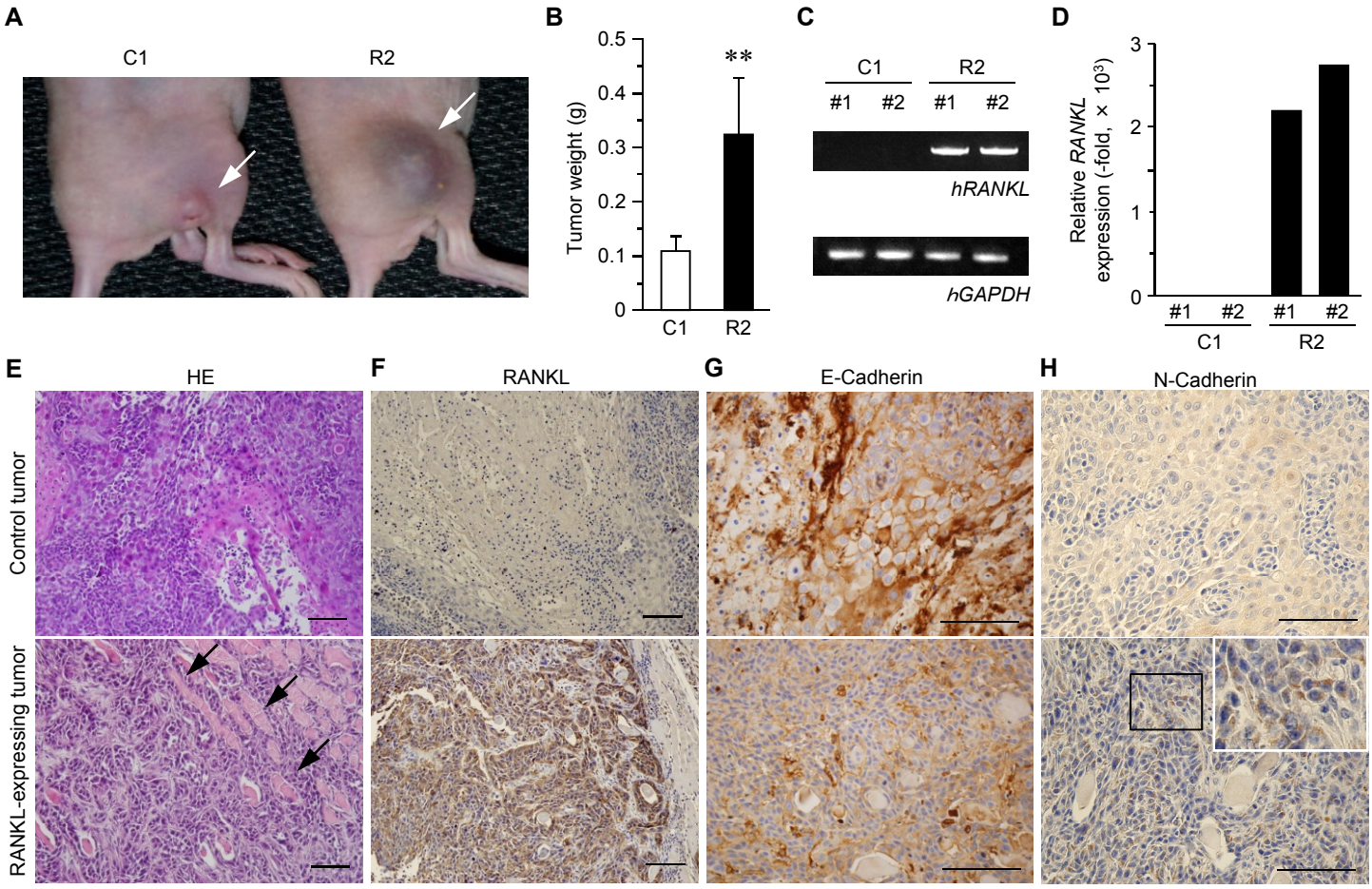

Figure 4 Yamada, T., *et al*.

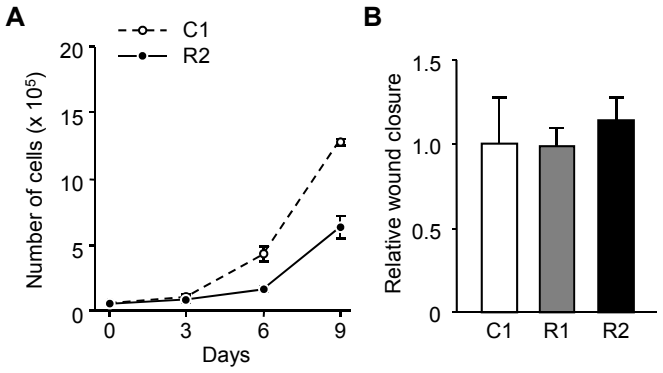

Figure 5 Yamada, T., *et al*.

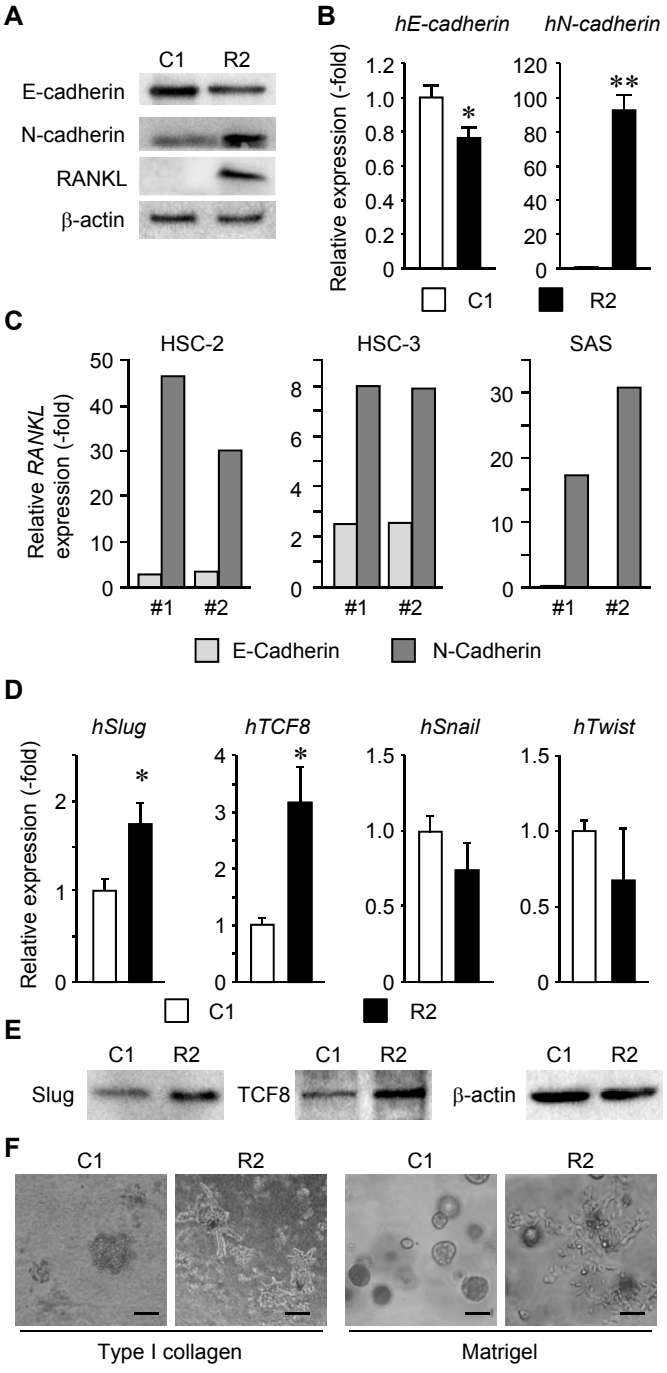

Figure 6 Yamada, T., *et al*.

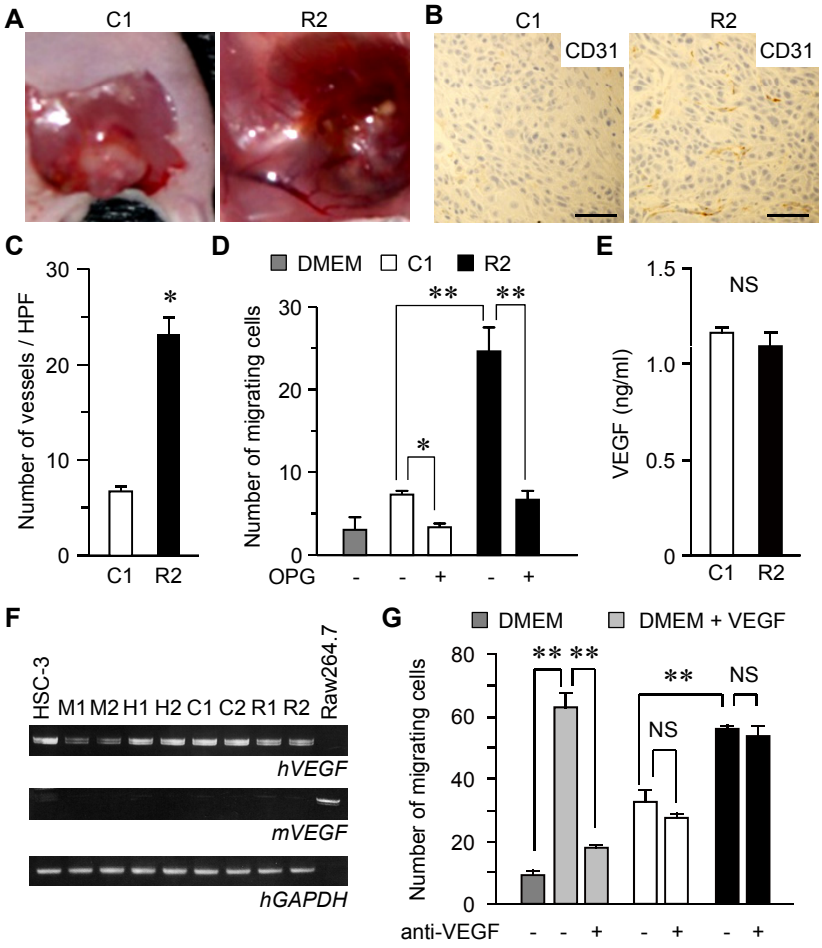

Figure 7 Yamada, T., *et al*.